JOURNAL OF GEOPHYSICAL RESEARCH, VOL. 100, NO. B3, PAGES 4079–4095, MARCH 10, 1995

Seismic refraction measurements within the Peninsular terrane, south central Alaska

Elizabeth L. Ambos
Department of Geological Sciences, California State University at Long Beach

Walter D. Mooney and Gary S. Fuis
U.S. Geological Survey, Menlo Park, California

Abstract. We present an interpretation of crustal seismic refraction data from the Peninsular terrane, one of the many exotic terranes that have been accreted to the continental margin of southern Alaska in the past 200 m.y. A seismic refraction line was collected along the Glenn Highway in the Copper River Basin of south central Alaska in 1984 and 1985, as part of the U.S. Geological Survey Trans-Alaska Crustal Transect (TACT) program. *P* wave velocities of 2.7-3.5 km/s and thicknesses of 1-2 km characterize post-Lower Jurassic sedimentary rocks that underlie most of the seismic refraction line. An average crustal velocity structure includes the following five velocity divisions. Beneath the sedimentary rocks lie 1-2 km of 4.0-4.6 km/s materials, correlating with andesitic volcaniclastic sedimentary rocks and lava flows of the Lower Jurassic Talkeetna Formation. Below these rocks, seismic velocity increases rapidly, from 5.0 to 6.1 km/s, in 2-3 km. At 7-8 km depth, velocity jumps to 6.3 km/s and increments to 6.6 km/s by 10-12 km depth. Velocities increase from 6.8 to 7.0 km/s between 12 to 20 km depth. At about 22 km depth, a jump in velocity from 7.0 to 7.4 km/s is inferred but is poorly resolved. Depth to the Moho discontinuity could not be determined from our data. The absence of clear *PmP* reflections may indicate that Moho is deeper than 40 km. Data from two offset shotpoints northeast of the line and within the Wrangellia terrane constrain the deep structure transition between Peninsular and Wrangellia terranes. The 6.3-6.6 km/s material thickens to the northeast, toward the suture between Peninsular and Wrangellia terranes, but southwest of its mapped trace at the West Fork fault. Peninsular terrane crustal structure appears dissimilar to that of continental interiors. It is similar to velocity structures determined for accreted island arc fragments in California, such as the basement of the Great Valley and the Klamath Mountains.

Introduction

Southern Alaska is a mosaic of oceanic and continental crustal fragments. These fragments have accreted to the continental margin of North America in the past 200 m.y. [*Coney et al.*, 1980; *Jones et al.*, 1982]. South of the Denali fault, *Jones et al.* [1981, 1984] have identified as many as 17 individual, fault-bounded terranes (larger terranes shown in Figure 1). Each terrane exhibits a characteristic stratigraphy documenting a geologic history distinct from that of its neighbors. Paleomagnetic studies conducted on rocks from many terranes in Alaska show that they are allochthonous, with several terranes originating far south of their present locations [e.g., *Bol*, 1993; *Hillhouse and Gromme*, 1984; *Plumley et al.*, 1982, 1983].

Knowledge of the crustal structure beneath terranes and across terrane boundaries is essential to understanding how terranes accrete and, ultimately, how continents are constructed. In this paper, we present results of seismic refraction/wide angle reflection profiling conducted chiefly within the Peninsular terrane in south central Alaska. A 160-km-long profile was recorded along the west part of the Glenn Highway in the Copper River Basin. This work was undertaken as part of the Trans-Alaska Crustal Transect (TACT) program of the U.S. Geological Survey and provides some of the first measurements of the crustal structure of the Peninsular terrane and its eastward transition to the Wrangellia terrane. Detailed information concerning the crustal structure within the Wrangellia terrane is provided by another seismic refraction/wide angle reflection profile, recorded along the east part of the Glenn Highway (also known as the Tok Cut-off) in the Copper River Basin. Results from this profile are documented by *Goodwin et al.* [1989]. Results from seismic lines intersecting the two profiles collected along the Glenn Highway provide further information on the structure of the Wrangellia terrane and terranes to the south and north. These data are reported by *Flueh et al.* [1989], *Fuis et al.* [1991], *Wolf et al.* [1991], and *Beaudoin et al.* [1992].

Paper number 94JB02621.
0148-0227/95/94JB-02621$05.00

Geological and Geophysical Setting

The Peninsular and Wrangellia terranes, together with the Alexander terrane to the southeast, are variously termed the

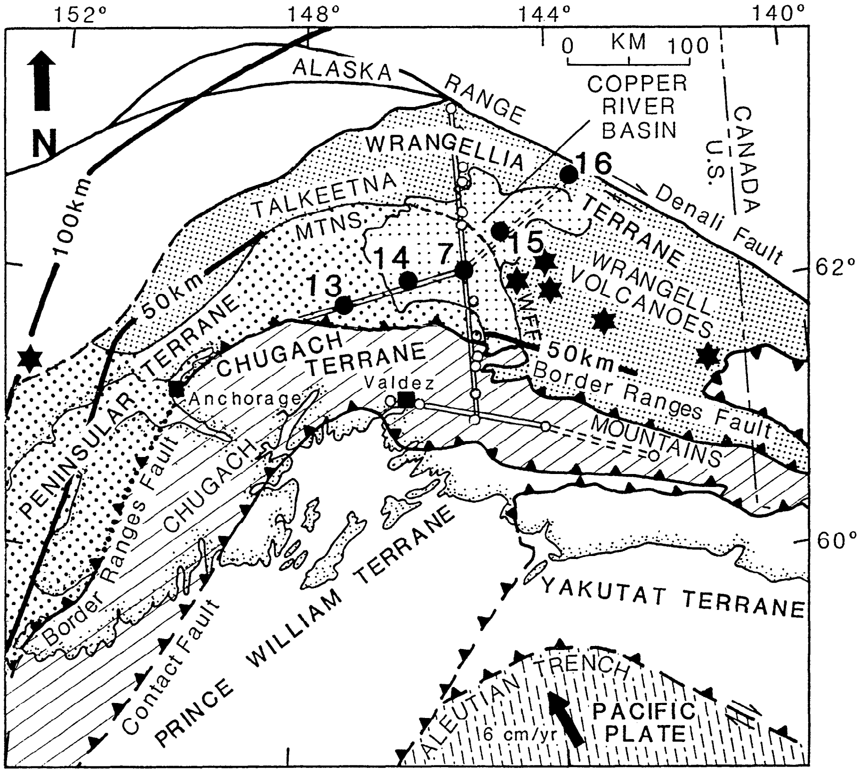

Figure 1. Map of south central Alaska showing the location of the seismic refraction profile (double solid and dashed line and associated solid circles) discussed in this paper. Dashed part of seismic profile indicates shot points offset from the seismometer deployment; this part is the subject of *Goodwin et al.* [1989]. Solid numbered circles indicate shot point locations. Other double lines and open circles are seismic profiles discussed by *Fuis et al.* [1991]. Key tectonostratigraphic terranes and suture zones [from *Jones et al.*, 1984], are identified. WWF is the abbreviation for West Fork Fault. Also shown are arc volcanoes (stars) and isobaths (heavy lines) of Aleutian and Wrangell Benioff zones [from *Stephens et al.*, 1984].

Talkeetna superterrane [*Csejtey et al.*, 1982; *Saleeby*, 1983; *Plafker et al.*, 1989], the southern Alaska superterrane (SAS) [*Panuska et al.,* 1990] or the Alexander-Wrangellia-Peninsular terrane (AWP) [*McClelland et al.,* 1992]. Within the study area (Figure 1), the Wrangellia and Peninsular terranes are bounded on the north by the Denali fault and on the south by the Border Ranges fault system [*Plafker et al.*, 1989]. Most of the seismic refraction data were collected within the Peninsular terrane. Offset shots were fired in the Wrangellia terrane and recorded in the Peninsular terrane. The data were collected in the Copper River basin, a lowland rimmed by the Wrangell Mountains to the southeast, the Chugach Mountains to the south, the Talkeetna Mountains to the northwest, and the Alaska Range to the north. The tectonic setting of the experiment is complex. The profile is located in the axial region of the Alaska orocline where Wadati-Benioff zone seismicity trends change, and a gap in arc volcanism exists [*Stephens et al.*, 1984; *Page et al.*, 1989; *Plafker et al.*, 1989].

The oldest exposures of Peninsular and Wrangellia terrane rocks are Paleozoic and Mesozoic in age. Most of these rocks formed in island arc settings. The Wrangellia terrane is characterized by Pennsylvanian to Permian and possibly older arc sequences topped by a thick Triassic flood basalt (Nikolai greenstone), which is in turn capped by Mesozoic sedimentary rocks [*Plafker et al.*, 1989]. The Peninsular terrane is part of a Mesozoic island arc, built on a basement of metasedimentary and metavolcanic rocks [*Burns*, 1985; *Plafker et al.*, 1989]. From south to north (Figure 2), the Peninsular terrane consists of the Tonsina ultramafic-mafic suite (Early or Middle Jurassic, appears only to the east of the area covered in Figure 2) [*Winkler et al.*, 1981; *DeBari and Coleman,* 1989], the Nelchina River Gabbronorite (Early or Middle Jurassic) [*Burns*, 1983, 1985; *Plafker et al.*, 1989], and the Talkeetna Formation (Lower Jurassic), consisting of andesitic and lesser basaltic volcaniclastic and marine sedimentary rocks [*Winkler et al.*, 1981; *Plafker et al.*, 1989]. The Tonsina ultramafic-mafic suite and the Nelchina River Gabbronorite are part of a belt of ultramafic and mafic rocks that extends westward along the south margin of the Peninsular terrane. These rocks are referred to as the Border Ranges ultramafic-mafic assemblage [see *Plafker et al.*, 1989]. The Tonsina suite and the Nelchina River Gabbronorite have closer affinities to island arc rocks than to mid-ocean ridge rocks and have crystallized at high pressures [*De Bari and Coleman*, 1989], suggesting that they have been exhumed from relatively deep crustal levels. In other parts of the Border Ranges ultramafic-mafic assemblage, nearly coeval, but intermediate plutonic rocks make up a significant percentage of the outcrops [*Burns*, 1985]. Intermediate plutonic rocks also intrude the Talkeetna Formation, and the latter is extensively faulted and folded. Mesozoic and Cenozoic sedimentary rocks overlie the Talkeetna Formation in the Copper River basin.

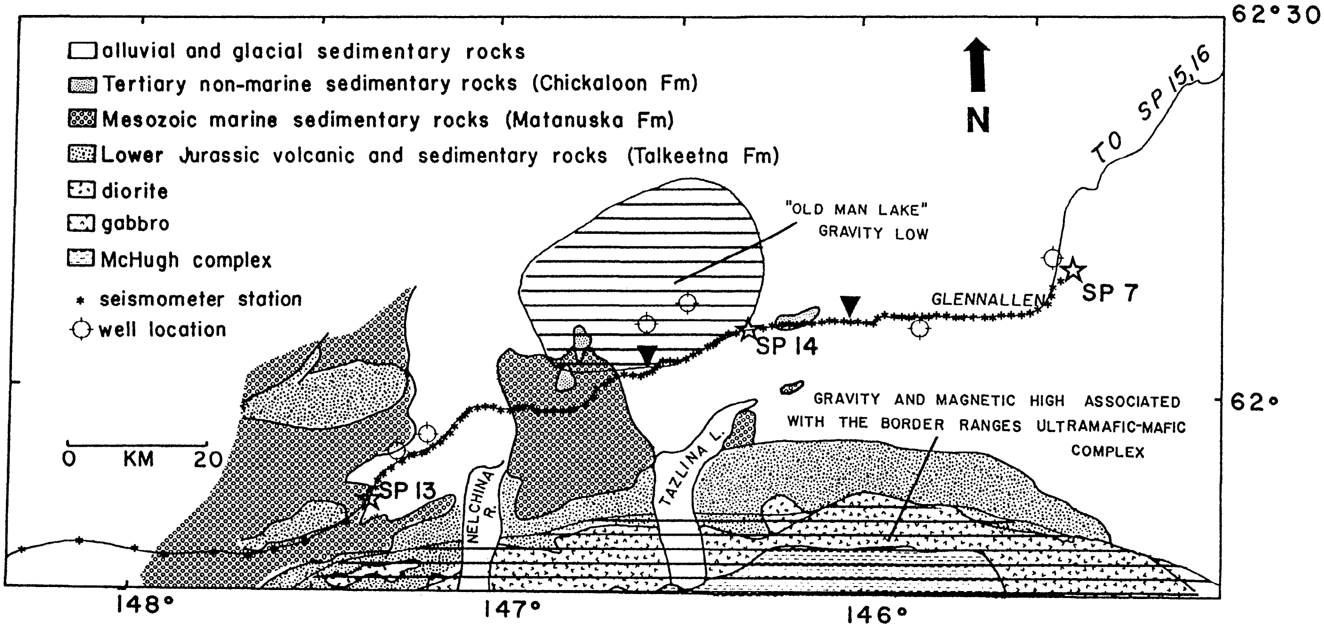

Figure 2. Expanded view of area surrounding in-line portion of the seismic line. Small asterisks are seismometer locations, stars are shot point (SP) locations. Region between two large triangles denotes limits of dense seismic survey surrounding SP 14. Heavy horizontal-lined sections show locations of prominent gravity and magnetic anomalies. Geologic contacts and simple Bouguer gravity and magnetic intensity anomalies are after *Andreason et al.* [1964] and *Burns* [1982]. Note that the gabbro listed in the legend is part of the Nelchina River gabbronorite of the Border Ranges mafic-ultramafic assemblage. The McHugh complex is a melange and is the northernmost part of the Chugach terrane, separated from the Nelchina gabbronorite by strands of the Border Ranges fault.

Paleomagnetic data from both the Wrangellia terrane [*Hillhouse*, 1977; *Jones et al.*, 1977] and Peninsular terrane [*Packer and Stone*, 1974; *Stone and Packer*, 1977] indicate that these terranes have moved northward thousands of kilometers relative to the North American craton since the early Mesozoic. Based on published paleomagnetic measurements [*Hillhouse and Gromme*, 1984] and geologic evidence [*Coney et al.*, 1980; *Csejtey et al.*, 1978, 1982; *Plafker et al.*, 1989] amalgamation of the two terranes occurred by Middle Jurassic to mid-Cretaceous(?) time. Accretion of the amalgamated Peninsular and Wrangellia terranes to the North American continent occurred by the mid-Cretaceous. Much of the area encompassed by the Copper River basin was formerly a forearc basin, at least during the Late Cretaceous when the Matanuska Formation was deposited [*Kirschner and Lyon*, 1973; *Grantz and Kirschner*, 1976]. The Copper River basin is related to the Cook Inlet basin [*Fisher and Magoon*, 1978], but is separated from it by the currently active right-lateral Castle Mountain fault system [*Lahr et al.*, 1986].

The published seismic refraction data collected onshore in Alaska prior to the TACT experiments are summarized by *Berg* [1973]. These early investigations [*Hales and Asada*, 1966; *Hanson et al.*, 1968] defined a three to four layer crust of 30-50 km total thickness, with most of the crust composed of 6.7-6.8 km/s material.

Gravity and magnetic surveys have previously provided better coverage onshore than the seismic data [*Woollard et al.*, 1960; *Andreason et al.*, 1964; *Barnes*, 1977; *Burns*, 1982; *Campbell and Barnes*, 1985; *Campbell and Nokleberg*, 1985, 1986]. Near the Glenn Highway seismic profile two major potential field anomalies have been identified (Figure 2). North of the central part of the profile, a gravity minimum, termed the Old Man Lake low, has been identified by *Andreason et al.* [1964]. South of the seismic profile, a gravity and magnetic high, corresponding to the Border Ranges mafic-ultramafic assemblage and intermediate intrusive rocks has been studied by *Burns* [1982, 1985] and *Campbell and Barnes* [1985]. Burns concludes that the magnetic anomaly can be modeled by a 3-6 km-thick body characterized by moderate to steep dips for its north and south flanks. *Campbell and Barnes* [1985] modeled gravity and magnetic data along a north-south profile through the east end of the Glenn Highway line. They conclude that a dense, magnetic body, possibly associated with the Border Ranges ultramafic-mafic assemblage, also underlies the Peninsular terrane, beneath the Copper River basin.

Data Collection and Analysis

Six seismic record sections recorded along the Glenn Highway profile using 120 portable U.S. Geological Survey (USGS) seismographs form the basis for this study. Five of the sections were recorded in 1984; the sixth was recorded in 1985. Shot times, locations, sizes, and data enhancement procedures are described in detail by *Daley et al.* [1985] and *Wilson* [1987] for the 1984 data and *Wilson et al.* [1987] for the 1985 data.

Each seismograph consisted of a 2-Hz vertical geophone whose output was recorded in multiplexed FM format on a cassette tape at three gain levels. Timing was provided by internal chronometers which were set to a master clock (accurate to 0.005 s) before the shot time, and were tested for clock drift after the seismographs were retrieved. The analog data were digitized at 200 samples/s. More detailed descriptions of USGS seismic refraction data collection procedures are available from *Blank et al.* [1979] and *Healy et al.* [1982].

In 1984 three shots were fired within the seismograph array, and two offset shots were fired northeast of the array. These shot points (SP) are numbered, from west to east, as SPs 13, 14, 7, 15, and 16 (Figure 1). The seismographs were spaced at 1-km intervals between the in-line shot points, increasing to 5 km spacing west of SP 13. In 1985, a single shot was recorded by a split-spread centered on SP 14. In this case, a seismograph spacing of approximately 250 m was used to obtain improved resolution of the shallow structure. Also in 1985, at a shot point near SP 13 (SP 23), an offset shot was fired into the Tok Cut-off line. This shot provides reversed coverage when combined with data from shotpoint 16, for the deep structure beneath the Glenn Highway line [see *Goodwin et al.*, 1989]. Sources consisted of drill holes, each 45 m deep and loaded with 800 to 2000 kg of ammonium nitrate explosives. Seismograph and shot point locations are accurate to approximately 30 m.

The data were modeled primarily using two-dimensional ray tracing. The ray tracing method is described by *Cerveny et al.* [1977]. Our modeling procedure consists of combining one-dimensional velocity models calculated from each shot point and iteratively perturbing this initial combined model until it successfully predicts the arrival times for all five shot points to within 0.05 s. In some cases, occasional mismatches of 0.1 s occur. *Walter and Mooney* [1982] provide an additional description of the modeling techniques.

The amplitudes of the seismic phases provide important constraints on the forward modeling process and have been modeled using the asymptotic ray theory as formulated by *McMechan and Mooney* [1980]. In addition, the 1985 split-spread profile centered around SP 14 was analyzed using two-dimensional ray tracing, synthetics calculation, and a semiautomated inversion procedure based on the assumption of planar-dipping structure [*Milkereit et al.*, 1985]. Our use of asymptotic ray theory to model the data means that the high-frequency approximation is used, and wave effects are not modeled.

The forward modeling process does not easily lend itself to error analysis and does not produce unique solutions, although evidence exists which indicates the general robustness of the approach [*Blundell*, 1984]. Nonetheless, several first-order statements concerning the degree of constraint of the model (Figure 3) are possible, based on careful monitoring of the iterative modeling process. The least constrained parts of the model are northeast of and directly beneath SP 7 and southwest of and directly beneath SP 13. Data collected along the Tok Highway in 1985 have extended constraints to the northeast of SP 7 over what is shown here [see *Goodwin et al.*, 1989]. Data collected along the Richardson Highway in 1984 extend velocity structure constraints to the north and south of SP 7 [*Fuis et al.*, 1991].

In the regions sampled by the rays, the velocity structure between zero (0) and approximately 5 km depth permits overall velocity variation of approximately 0.1 km/s and interface depth variation of approximately 0.2 km. Deeper in the section, particularly within and below the poorly defined LVZ indicated at 6-8 km depth, constraints deteriorate to possible variations of 0.2 km/s in *P* wave velocity and 0.5-1 km in depth. These error estimates are taken from observation of the many trial models tested

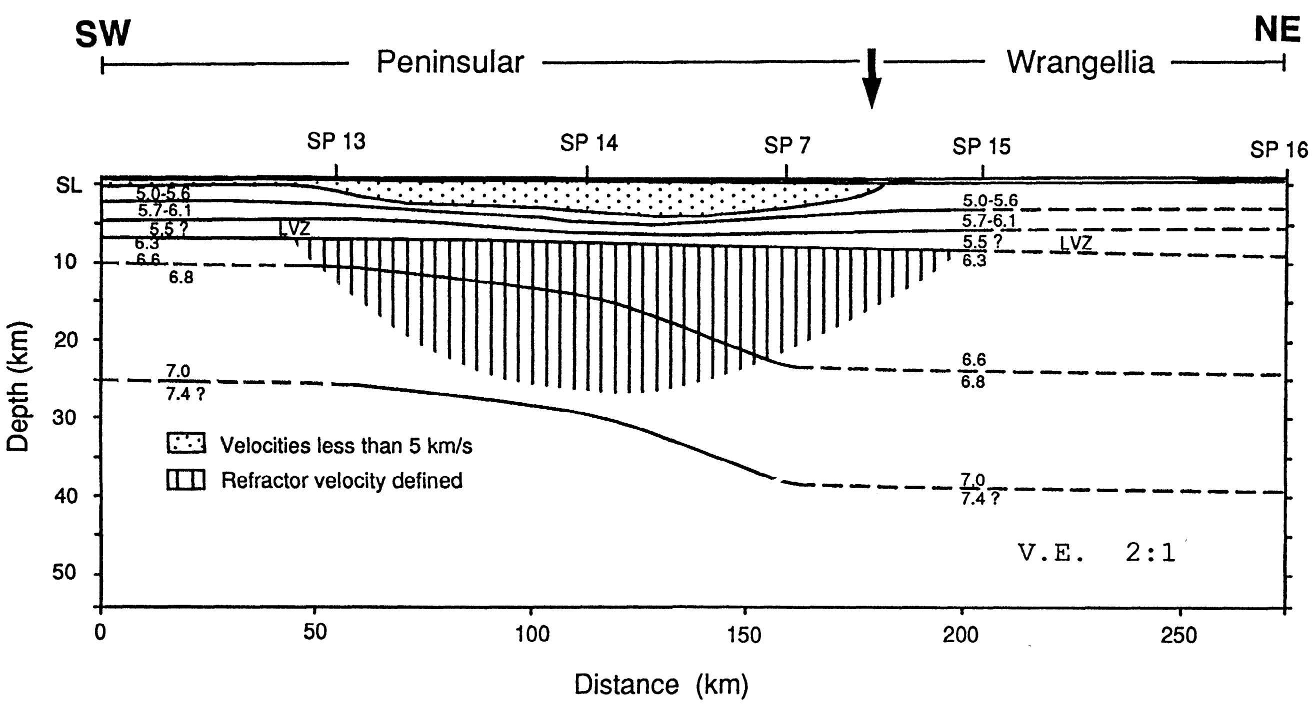

Figure 3. *P* wave velocity field derived for the Glenn Highway seismic profile. Boldface numbers are *P* wave velocities in kilometers per second. Dashed lines indicate boundaries that are unconstrained by this data set. Areas of good velocity control for the mid to lower crust (heavy vertical lines) are also indicated, and were derived from examination of the raytracings for each shotpoint. Note that the "LVZ" in the midcrust is only well-defined in a region between SPs 14 and 13.

during the ray tracing modeling and thus must be considered only qualitative determinations. Direct inversion of the data was not feasible for most of the data as factors such as too widely-spaced stations and violation of planar structure constraints would have limited the utility of these methods [e.g. *Liu and Stock*, 1993; *Shaw*, 1992; *Zelt and Smith*, 1992].

Results and Discussion

Velocity Structure of the Copper River Basin

Interpretation of the structure beneath the Copper River basin is aided by stratigraphic and sonic velocity logs from several oil exploration wells near the seismic line [*Alaska Geological Society*, 1969], proprietary seismic reflection data released to the USGS (R. Shafer, written communication, 1985), gravity and magnetic modelling [*Andreason et al.*, 1964; *Burns*, 1982; *Campbell and Barnes*, 1985] and geologic mapping in the area [*Burns*, 1985; *Winkler et al.*, 1981; *Grantz*, 1960, 1961, 1964, 1965; *Plafker et al.*, 1989]. Using these data, the short-range (less than 20 km offset) refraction data (Figure 4) may be interpreted in the following way (Figure 5).

Tertiary and younger section. Traveltime branches of variable *P* wave velocity (1.7 km/s at SP 7, 2.1 km/s at SP 14, and 2.8 km/s at SP 13) are observed to 1-2 km range (Figure 4). These branches are most clearly defined in the closely spaced (250-m station spacing) deployment around SP 14 (Figure 6). This surface layer corresponds to 200-400 m of glacial and alluvial sediments, underlain by undifferentiated Upper Tertiary and the Paleocene nonmarine, relatively unconsolidated sediments of the Chickaloon Formation. The primary evidence for this correlation comes from the stratigraphic and sonic logs from adjacent oil exploration wells (Figure 5).

The increase in surficial velocity to the southwest, toward SP 13, may reflect the absence of the glacial and alluvial deposits, as mapping indicates that they become locally patchy to the west (see Figure 2). Alternatively, the velocity increase may correlate with the observed southwestward increase in induration of Tertiary sedimentary rocks along the southern margin of the basin [*Grantz and Fay*, 1964].

Upper Cretaceous Matanuska Formation and older Mesozoic rocks. East of SP 14 and below the Tertiary and younger section lies a 1-2 km thick section with a velocity of 2.5 km/s at its top and about 3.0-3.5 km/s at its base. These velocities are determined from the first-arrival branches observed to ranges of 2-11 km for SPs 14 and 7.

From comparison with well log information [*Alaska Geological Society* (AGS), 1969] this branch correlates with sedimentary rocks of the Matanuska Formation (defined by *Martin* [1926]), comprising Upper Cretaceous, predominantly marine, siltstone and sandstone. The velocity range of 2.7-3.5 km/s is within the range found for siltstones and sandstones [*Christensen*, 1982]. Either a first-order discontinuity in velocity or rapid increase in velocity gradient is indicated at the top of the Matanuska Formation. This discontinuity correlates with the unconformity observed between the Cenozoic sequence and the underlying Cretaceous sedimentary rocks [*Clardy et al.*, 1984; *Andreason et al.*, 1964].

Density measurements [*Andreason et al.*, 1964], sonic logs from the four wells along the line, and geologic evidence of greater induration in the Cretaceous strata [*Grantz and Fay*, 1964] are consistent with a higher velocity in the Matanuska than in the younger strata. Although the Chickaloon Formation and younger sedimentary rocks locally may reach 1.2-1.6 km thickness in the Matanuska Valley southwest of the Glenn Highway line [*Clardy et al.*, 1984], stratigraphic logs from oil exploratory wells closest to the Glenn Highway line indicate the presence of Matanuska Formation within 250 m of ground surface [*AGS*, 1969] (Figure 5a).

Below the Matanuska, thinner (several hundred meters maximum) and less extensive deposits of the Lower Cretaceous marine sedimentary rocks of the Nelchina and Kennecott Formations and Upper Jurassic sedimentary rocks of the Naknek, Chinitna, and Tuxedni Formations may be present, although the well log evidence is patchy (Figure 5). For example, the well situated halfway between SPs 7 and 14 reached the Nelchina Formation at approximately 1.8 km depth. These older sedimentary rocks are similar in composition to the overlying Matanuska Formation and cannot be distinguished from them on the basis of seismic velocity. Consequently, they may be included at the base of the 2.7-3.5 km/s velocity field segment. The 1-2 km thickness of this interval determined by the refraction data is in agreement with estimates of an average thickness of 1.5-1.8 km (C. E. Kirschner, personal communication, 1985) for the combined Matanuska Formation and older sedimentary rocks in this area.

Early Jurassic Talkeetna Formation. An interval with velocities increasing from approximately 4.0 to 4.6 km/s and varying in thickness from 0.5 to 2.0 km underlies the 2.7-3.5 km/s interval. A first-order discontinuity between the 2.7-3.5 km/s and 4.0-4.6 km/s intervals is indicated in the seismic refraction data. Arrival branches with apparent velocities in the 4.0-4.6 km/s range are observed over ranges varying from 7 to 15 km for all SPs (Figure 4).

Seismic reflection data from the Copper River basin show a reflector at a two-way travel time varying between 1 and 2 s, corresponding to 1.5-3.0 km depth (assuming an average interval velocity of 3 km/s). This reflector has been interpreted as the top of the boundary between the Matanuska Formation and possibly older Mesozoic units and the Talkeetna Formation (C. E. Kirschner, personal communication, 1985, R. Schafer, written communication, 1985). Sonic logs (Figure 5b) from Copper River basin wells also show an abrupt velocity increase near the proposed Matanuska-Talkeetna boundary, from 3 km/s average velocity, to 4-5 km/s. One interpretation is that this evidence indicates that the 4.0-4.6 km/s interval corresponds to the early Jurassic volcaniclastic sedimentary rocks of the Talkeetna Formation. Alternatively, the 4.0-4.6 km/s velocity material may represent an interval of Lower Cretaceous to Jurassic age marine sedimentary rocks (Naknek, etc., as discussed earlier), between the Matanuska and Talkeetna Formations.

One problem with the correlation of Talkeetna Formation with the 4.0-4.6 km/s velocity interval is that it relies on evidence from the stratigraphic logs. Often the formation identifications noted in the stratigraphic logs were made using small samples of material recovered near the base of the wells (C. E. Kirschner, personal communication, 1985). In addition, laboratory measurements of andesite breccia samples collected from the Talkeetna Formation (*Fuis et al.*, 1991; N. I. Christensen, personal communication, 1986) indicate velocities no less than 5.8-6.2 km/s for these

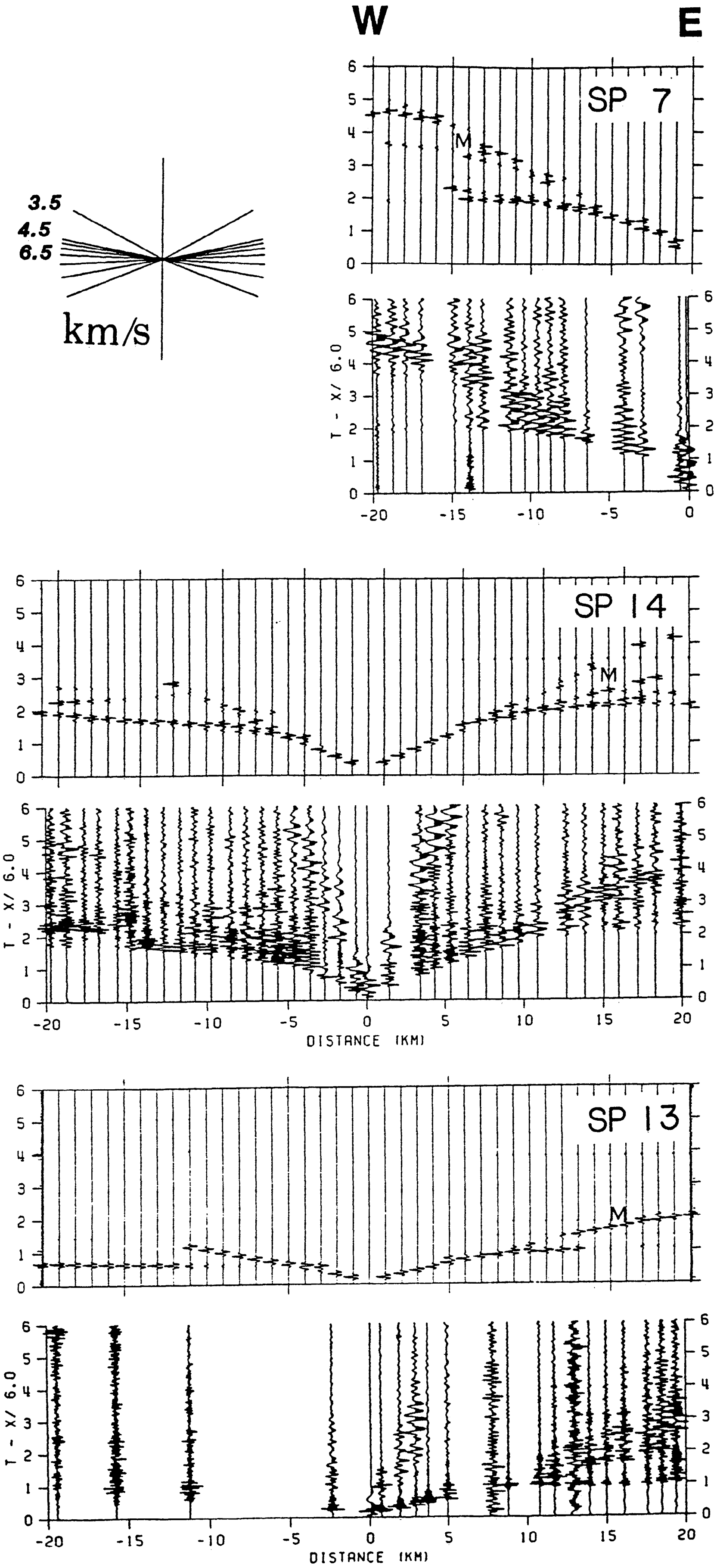
W
E
SP 7
M
3.5
4.5
6.5
km/s
T - X/ 6.0
SP 14
M
DISTANCE (KM)
SP 13
M
DISTANCE (KM)

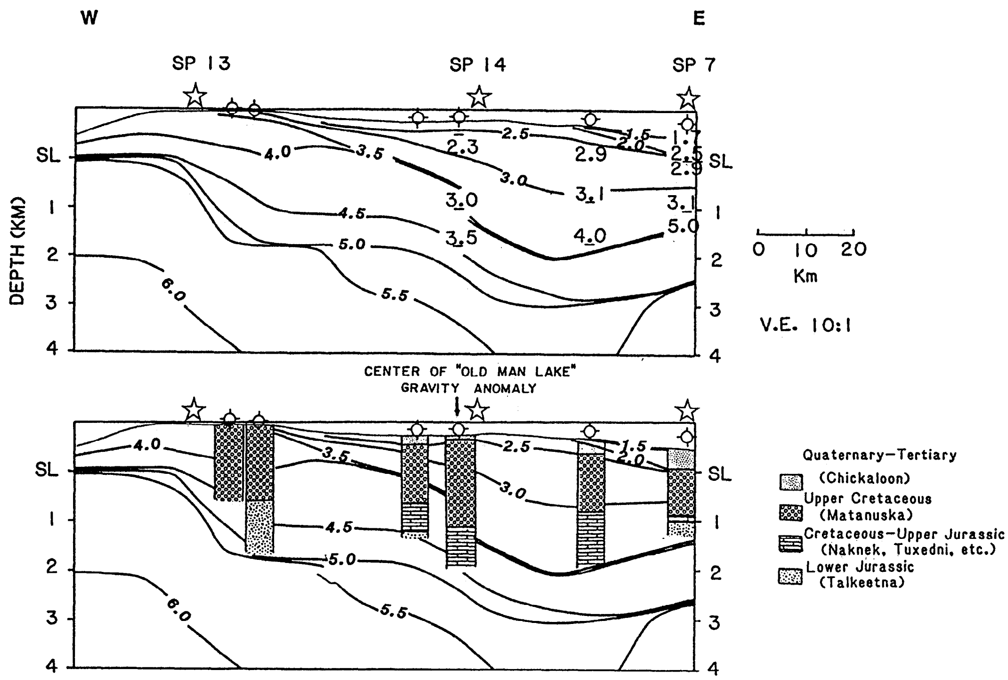

Figure 5a. *P* wave velocity field (small numbers in italics are ray trace velocities) along the Glenn Highway seismic profile derived from two-dimensional ray trace modeling for the upper 5 km. (top) Averaged sonic log information for three wells along the profile (large numbers not in italics). (bottom) Stratigraphic well-log information [after *Alaska Geological Society*, 1969].

materials. These laboratory velocities are far higher than those measured in the seismic refraction data (4.0-4.6 km/s). The direct correlation of Talkeetna Formation laboratory sample measurements with the 4.0-4.6 km/s seismic refraction velocities is therefore problematic. Our preferred interpretation is that the seismic refraction data measured the upper part of the Talkeetna Formation, which is formed mostly of sedimentary rocks [*Burns*, 1985].

Lateral changes in Copper River basin velocity structure. Several lateral transitions observed in the velocity structure within the Copper River basin (Figure 5) appear to correlate with changes observed in the geology and/or potential field data. The Old Man Lake gravity anomaly mentioned earlier is a broad Bouguer gravity low centered to the north of SP 14 (Figure 2) and is interpreted by *Andreason et al.* [1964] as a localized thickening of Copper River basin sedimentary strata. This thickening might represent the depocenter for the basin area in the Mesozoic. It could also be the result of tectonic thickening by folding or thrust faulting. The former possibility seems more likely as well logs from the Old Man Lake anomaly region (Figures 2 and 5) appear to contain the oldest basinal sediments (C. E. Kirschner, personal communication, 1985).

Thickening of the 3.0-3.5 km/s (Matanuska and older) material takes place just east of SP 14 (Figure 5) and is well-defined by the asymmetry of first arrivals for both the 1984 data (Figure 4) and the 1985 densely-spaced survey (Figures 6 and 7). Therefore the thickest part of the basin, as defined by the seismic refraction data, is offset to the northeast from the minimum gravity anomaly values. This discrepancy could be explained by the sparsity of observations used in constructing the gravity anomaly contours [*Andreason et al.*, 1964]. In agreement with the refraction results, the well closest to SP 14 shows the thickest section of Matanuska Formation. The thickness found in this bore hole is greater and the sonic velocities lower (by about 0.5-1.0 km/s) than indicated by the refraction data. This discrepancy may possibly be due to the projection of the well onto the seismic refraction line from 10 km to the north, where Copper River Basin sedimentary rock thicknesses may be greater (Figures 2 and 5).

Farther to the southwest, in the vicinity of SP 13, the interval of material with velocities less than 3.5 km/s thins abruptly (Figure 5). SP 13 is located in Tahneta Pass, an area marked by outcrops of Matanuska and Talkeetna Formation rocks. The two wells nearest SP 13 indicate the presence of Matanuska Formation, but at a higher velocity than to the northeast, due to changes in composition or metamorphism. *Andreason et al.* [1964] suggest a southwesterly increase in mafic constituents in the Matanuska

Figure 4. (Opposite) Record sections and asymptotic ray theory synthetics for the three in-line shotpoints for offsets less than 20 km. From top to bottom, SPs 7, 14, and 13 are shown, with synthetic record section placed above the data section. The "M" labels on the synthetic record section indicate approximate locations of multiply refracted arrivals. The velocity rosette in the top left-hand corner provides a reference frame for the velocities that may be observed in the record section. All record sections are reduced time (T-D/6) and trace-normalized. A Ricker wavelet (10-Hz frequency) was used as the source pulse in calculating the synthetics.

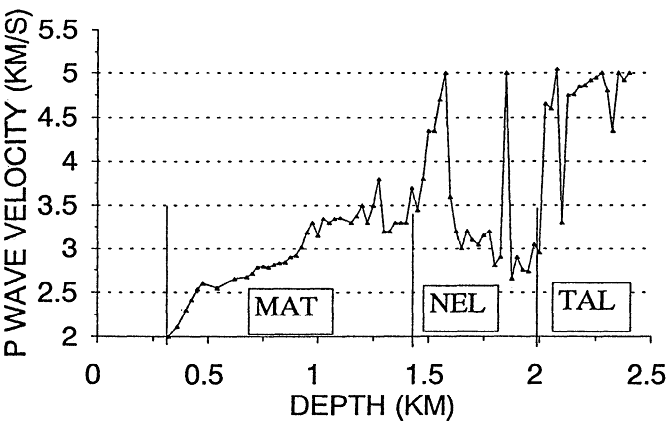

Figure 5b. Sample raw stratigraphic and sonic well log data, from the Ahtna #1 well (located near SP 7). The designations "MAT", "NEL", and "TAL" refer to the Matanuska, Nelchina, and Talkeetna Formations, respectively. These identifications were supplied with the original stratigraphic logs.

Formation. Alternatively, increasing induration in the sediments, such has been noted in surficial mapping [*Grantz and Fay*, 1964; A. Grantz, personal communication, 1986], and/or the presence of igneous intrusives or hornfels-facies Talkeetna Formation rocks (G. Plafker, personal communication, 1988) may cause the southwestward increase in velocities. Although the travel time curve to the southwest of SP 13 is defined by only a few scattered stations (Figures 2 and 4), the asymmetry of the split spread is unmistakeable. Materials with velocities less than 3.5 km/s must thin abruptly southwest of SP 13.

The persistent southwestward increase in the sedimentary rock velocities from the Copper River basin toward the Matanuska valley is documented not only in the increase in apparent velocities observed in the first arrival branches to the southwest, but also in the free surface, multiply-reflected refractions within the 2.7-3.5 km/s interval (see Figure 4, compare SP 7 and SP 13). These multiples have been noted in other sedimentary basins characterized by high-velocity gradients and provide strong additional constraints on the velocities modeled [e.g., *Hwang and Mooney*, 1986; *Fuis et al.,* 1991].

Detailed definition of the velocity structure near SP 14. In 1985, 120 vertical component seismometers were deployed at 250-m spacing in a split-spread profile on either side of SP 14 (Figure 2). This spatially denser set of observations was analyzed using the two-dimensional slant-stack inversion algorithm of *Milkereit et al.* [1985]. Comparison of crustal structure determined through forward modeling with that determined with this inversion scheme provides an important check on the overall robustness of the forward modeling approach. The data were initially modeled through detailed ray tracing and calculation of predicted arrival times and synthetic seismograms (Figure 6), similar to the techniques used in the analysis of the 1984 data. Each side of the split spread was then transformed from the X-T (travel time-distance) domain (Figure 6) to the tau(τ)-p (delay or intercept time-ray parameter (also referred to as horizontal slowness)) domain (Figure 7a). This transformation is actually a resampling of the information contained in T-X displays (record sections such as Figure 6) in that for a range of intercept times, trace amplitudes are summed along lines of constant ray parameter. The resulting display in the tau-p domain may clearly separate reflected and refracted arrivals, allowing for easier data interpretation.

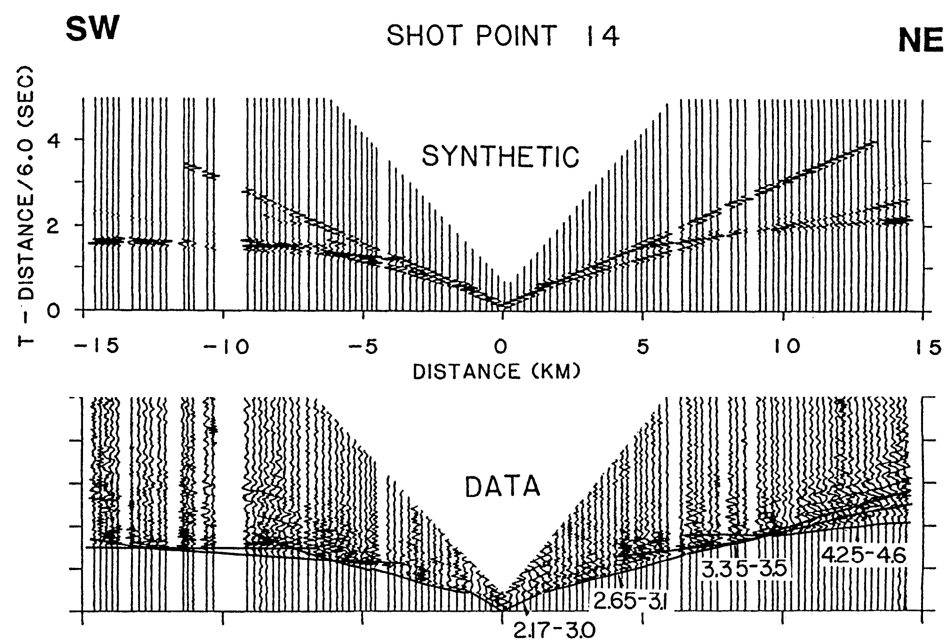

Figure 6. Record section of the densely spaced experiment conducted in the vicinity of SP 14 in 1985, compared to asymptotic ray theory synthetics (top) determined using forward modeling. Note the obvious asymmetry of the travel time curve on either side of the shot point. These synthetic seismograms include only primary reflected and refracted arrivals, no multiples or converted phases. The mismatch of some of the secondary phases between predicted and observed is thus not fully explained.

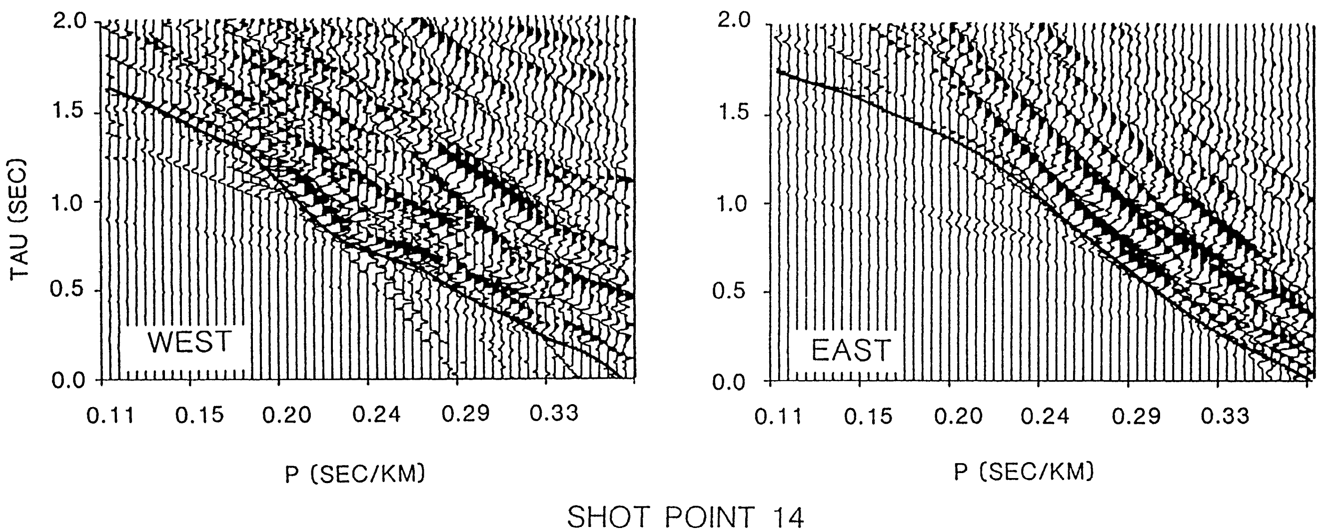

Figure 7a. Slant stacks of the densely spaced 1985 split-spread survey, with tau-p picks (solid lines) used for the automatic inversion procedure superimposed. The east and west sides of the split-spread are shown separately.

The τ-p curves were fit to the data through an iterative cross-correlation procedure [*Milkereit et al.*, 1985], and a dipping-layer solution was calculated. The resulting solution for structure directly beneath the shot point is compared to the best fit structure derived from forward modeling, as are dips determined for corresponding layers for the two methods (Figure 7b). Apart from a difference of 0.4 km/s in starting velocity between forward modeled and inversion results, the maximum difference at any one point between the two curves is approximately 0.2 km/s. The major differences between the two solutions lie in the apparent smoothing of first-order discontinuities by the inversion method and the sudden perturbations in the dip determination curve, both of which have been shown by *Milkereit et al.* [1985] to be artifacts of the inversion scheme. The differences may also result from lateral velocity variations (outside of the constraint of planar dipping layers) not taken into account in the inversion process. The advantage of the slant stack inversion is that it can rapidly define the velocity-depth structure for a sequence of gently (less than 8°) dipping layers. The disadvantage of the method is that it is most useful for long-offset seismic sections characterized by dense (<1 km separation) station spacings.

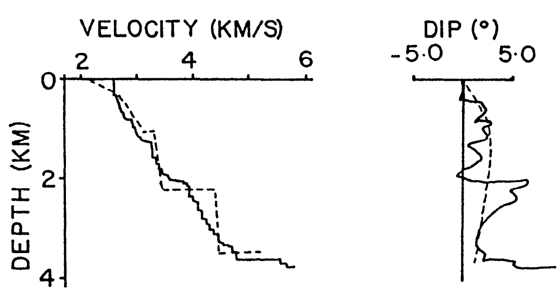

Figure 7b. (left) Comparison of the velocity-depth functions derived from slant stacking and direct inversion of the 1985 data, and that determined from forward modeling. (right) Comparison of the layer dips directly determined using the two methods. For both diagrams, the dashed line indicates the forward modeling interpretation, the solid line, the inversion determination.

Velocity Structure of the Middle to Lower Crust

Below the 4-4.6 km/s interval, which we identified as either the Talkeetna Formation, or younger sedimentary rocks, lies 2-5 km of material with velocities of approximately 5.0-6.1 km/s (Figure 3). Arrival branches with apparent velocities in the 5.0-6.1 km/s range are observed at ranges of 10-55 km for SP 7, 15-35 km for the east side of SP 14, 12-25 km for the west side of SP 14, and approximately 8-35 km offset for SP 13 (Figures 3 and 6). As these materials lie below the range of the well logs, their compositions are less well-determined. They may represent Talkeetna Formation rocks, possibly intruded by diorite plutons, some of which crop out in the northern Copper River Basin [*Nokleberg et al.*, 1986]. This correlation could satisfy the velocities measured (e.g., *Fuis et al.,* 1991; N. I. Christensen, personal communication, 1986) although diorites are more commonly characterized by velocities in the 6.4 km/s range [e.g. *Birch*, 1960; *Beaudoin et al.*, 1992]. From mapping in the Talkeetna Mountains to the northwest, *Burns* [1985] determined that the Talkeetna Formation may be subdivided into a 3-km-thick upper part, comprising interlayered marine sediments and tuffs, overlying a 3-km-thick section of andesite flows and tuffs, grading at its base into basalt. If this definition is extrapolated to the Talkeetna Formation rocks in this study area, the division between 4.0-4.6 km/s and 5.0-5.8 km/s intervals may reflect this internal change in the Talkeetna Formation. This explanation is also consistent with the laboratory velocity measurements in the range of 5.8-6.2 km/s, for andesite flows and breccias from the Talkeetna Formation [*Fuis et al.*, 1991]. Although the Nelchina River gabbronorite (the part of the Border Ranges ultramafic and mafic assemblage directly south of the seismic line, see Figure 2) rocks are faulted and intruded structurally below the Talkeetna Formation [*Pavlis*, 1983; *Burns*, 1985], it is unlikely that they are represented at this interval, as velocities of 5.0 to

5.8 km/s are too low [e.g. *Christensen et al.,* 1975; *Fuis et al.,* 1991] for most mafic and ultramafic rocks.

Below the interval in which velocity increases from 5.0 to approximately 5.8 km/s lies a low-velocity zone (LVZ) with an approximate velocity of 5.5-5.7 km/s and thickness of 2 km. Of course, the velocity and thickness of the LVZ may be altered in various ways to satisfy the travel time and amplitude data. In practice, it is difficult to tell the difference between a thick LVZ with a velocity slightly less than the overlying section, and a thin LVZ with a velocity substantially (1 to 2 km/s) lower than the overlying section.

We should note that although some theoretical modeling [e.g., *Braile and Smith,* 1975] indicates that the reflection from the top of the LVZ is a strong constraint on LVZ structure, we do not find this to be the case with our data. The reflection from the top of the LVZ blends with the refractions from the layers below and above the LVZ. Instead, we find that the best evidence of the LVZ is the time offset in the travel time curve and associated high-amplitude postcritical reflection from the base of the LVZ. This reflection is observed at 15-40 km range west of SP 14 and at 20-40 km range west of SP 13 (Figure 8). This LVZ is *not* readily evident from SP 7 data or from the eastern side of the SP 14 split-spread (Figure 8), where the travel time curves are continuous. Thus the LVZ does not appear to be a laterally continuous feature (see Figure 3, also *Goodwin et al.* [1989]). The LVZ could represent a zone of increased pore pressure [*Walder and Nur,* 1984], granite sill(s), from a late intrusion event in the dioritic plutonism, a highly serpentinized portion of Nelchina complex rocks, or even

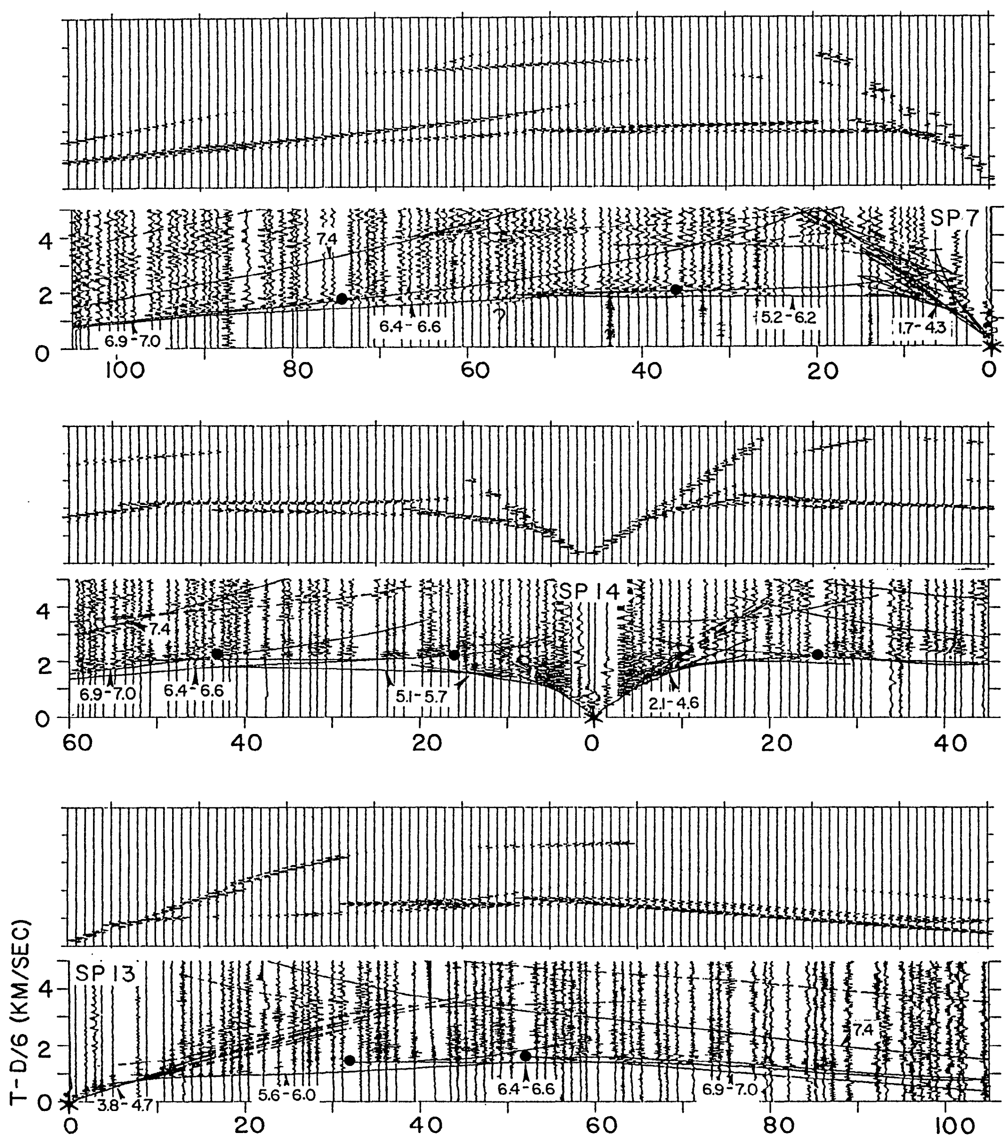

Figure 8. Record sections and asymptotic ray theory synthetics of the three in-line shotpoints, with travel time curves (with *P* wave velocities annotated) predicted from the ray trace modeling superimposed. All record sections are reduced time (T-D/6) and trace normalized. Question marks refer to zones where differences occur between predicted and observed travel times; these particular differences occur in areas where the seismic profile undergoes an abrupt change in azimuth (see Figure 2). Multiple branches are dashed, as are primarily reflected refractions. Dots signal the location of the critical point (precritical branches have been calculated for SPs 7 and 14).

layered metasedimentary rocks [e.g., *Christensen*, 1989]. The latter suggestion follows from *Burns*' [1985] observation that metasedimentary rocks are preserved as septa within the Border Ranges ultramafic-mafic complex.

Below the LVZ is a section of approximately 6.3-6.6 km/s velocity (note that although we state the interval as 6.3-6.6 km/s, our data do not constrain this interval to better than 0.2 km/s) ranging in thickness from 3 km to at least 15 km. The refraction arrival branch is observed from 38 to 90 km range for SP 7 and less clearly from 30 to 90 km range for SP 14 and from 32 to 88 km range for SP 13 (Figure 8). The corresponding lithology for that interval could again be granodiorite [*Birch*, 1960; *Christensen*, 1982], correlating with the presence of Jurassic granitic to dioritic rocks exposed in the northern Peninsular terrane [*Fuis et al.*, 1991; *Nokleberg et al.*, 1986, 1989]. Alternatively, this interval could be basalt [*Christensen et al.*, 1974], which is found at the base of the Talkeetna Formation [*Burns*, 1985]. Basalts of the Permo-Triassic Kamishak Formation, which crop out on the Alaska Peninsula, could also lie beneath the Talkeetna Formation in the Copper River Basin (A. Grantz, personal communication, 1986). High-grade metamorphic rocks, such as blueschists, are also candidates [e.g., *Iida et al.*, 1967]. The only rock types that can be discounted on the basis of velocity are most granites and sedimentary rocks, whose velocities are generally lower than 6.4-6.6 km/s [e.g. *Hughes and Maurette*, 1956; *Christensen*, 1982; *Beaudoin et al.*, 1992].

The 6.3-6.6 km/s interval is floored by a rapid increase in velocity (or first-order velocity discontinuity) to 6.8-7.0 km/s. The wide-angle reflection from this discontinuity begins at a range of 70 km for SP 7 and at a range of 50 km for SP 14 (Figure 8). Velocities greater than 6.7 km/s generally correlate with very high-grade metamorphic rocks, or mafic-ultramafic rocks. Therefore it is possible that the 6.9 km/s (average) interval corresponds to the gabbros of the Border Ranges ultramafic-mafic assemblage. This would mean that the depth to the complex increases to 11 km depth to the northeast, from its mapped expression to the south (Figure 2) of the Glenn Highway line. An increase in depth to the 6.9 km/s discontinuity is clearly indicated by the offset SPs 15 and 16 (Figure 3 and 9). There is also evidence from SP 7 that the 6.9 km/s discontinuity begins to deepen to the northeast between SPs 7 and 14.

Below the 6.8-6.9 km/s discontinuity velocity increases to approximately 7.0 km/s with a gradient of 0.013 s^{-1} (km s^{-1} km^{-1}). At depths of 20-30 km (Figure 3), velocity rapidly increases again. The velocity below the interface is poorly defined, although a velocity of 7.4 km/s has been assigned. The evidence for this discontinuity is contained mainly in a poorly defined wide-angle reflected phase (Figure 8, SPs 7 and 14; Figure 9, SP 16). We do not believe this reflection is *PmP*, as normal upper mantle velocities (7.8-8.2 km/s) cannot be present at those depths, or the arrivals predicted for the offset shot points become too early. Below the 6.9 km/s discontinuity, velocities probably increase to greater than 7.0 km/s, but without any discernable crust-mantle boundary. The latter boundary is therefore deeper than about 40 km. This result is confirmed in the work of *Goodwin et al.* [1989], and the implications are discussed in more detail there.

Seismic refraction and tectonic modeling results from studies conducted to the northeast and south of the West Glenn data [*Page et al.*, 1986; *Fuis et al.*, 1991; *Fuis and Plafker*, 1991] have proposed that the lower crust beneath the Peninsular terrane may either be the product of tectonic underplating during subduction *or* may have resulted from "thick-skinned" accretion of a 20+ km thick Peninsular terrance to North America. The results of the West Glenn seismic refraction line modeling do not clearly support either hypothesis.

Crustal structure transition between Peninsular and Wrangellia terranes. The northeast thickening of the 6.3-6.6 km/s interval, or, alternatively, the northeast dip of the 6.9 km/s (average) discontinuity, is the most significant feature of the deeper structure of the Peninsular terrane. At the west end of the Glenn Highway profile, the Peninsular terrane velocity structure is characterized by high velocity at relatively shallow depths, 6.8 km/s at 10-km depth. Within the Wrangellia terrane [*Goodwin et al.*, 1989] this high velocity is reached at much greater depths, 6.7 km/s at 19 km. Some of this thickening of the 6.3-6.6 km/s layer is accomplished between SPs 7 and 14.

The *Goodwin et al.* [1991] model of the Tok Highway seismic refraction data to the northeast of our study shows an abrupt change in **shallow** crustal structure at the West Fork fault system. Modeling of potential field data [*Campbell*, 1987] also show a boundary at this fault. This fault lies some 15-30 km northeast of SP 7 and is commonly identified as the suture between Peninsular and Wrangellia terranes [*Plafker et al.*, 1989].

This seeming discrepancy in location between the marked velocity changes in the shallow and deep layers is puzzling. If the strong lateral change in the deep layers is directly related to the suture between Peninsular and Wrangellia terranes, then that suture has a considerable spatial extent. Alternatively, the crustal structure transition may be due to intraterrane rather than interterrane differences. We may be seeing a change in deep crustal structure **within** the Peninsular terrane (i.e., a west to east thickening of the 6.3-6.6 km/s material). A velocity structure transition between Peninsular and Wrangellia terranes in the mid to lower crust can be explained in several ways. First, the Wrangellia terrane may be atop a continental crustal fragment [e.g., *Goodwin et al.*, 1989], whereas the Peninsular terrane has at its base oceanic crust or island arc plutonic material [*Fuis and Plafker*, 1991]. We can hypothesize that these differences persist to deeper crustal levels, so that more "continental" (lower average velocity) material is present beneath the Wrangellia terrane as compared to the Peninsular terrane, with the latter being more "oceanic" in nature. The presence of "oceanic" or more mafic crust beneath the Peninsular terrane would explain the relatively high magnetic signature of the terrane, as compared to Wrangellia [*Andreason et al.*, 1964; D. L. Campbell, personal communication, 1985].

A second hypothesis for the crustal structure difference is that it is somehow related to the current configuration of plate boundaries in the region. As pointed out earlier, arc volcanism and Benioff zone seismicity trends undergo a distinct change in the vicinity of the Glenn Highway seismic line (Figure 1). This tectonic change is consistent with the crustal structure change: the Benioff zone dips more steeply beneath the Wrangellia part of the profile, allowing for introduction of the magma that supplies the Wrangellia volcanoes and forms a presumed arc plutonic complex

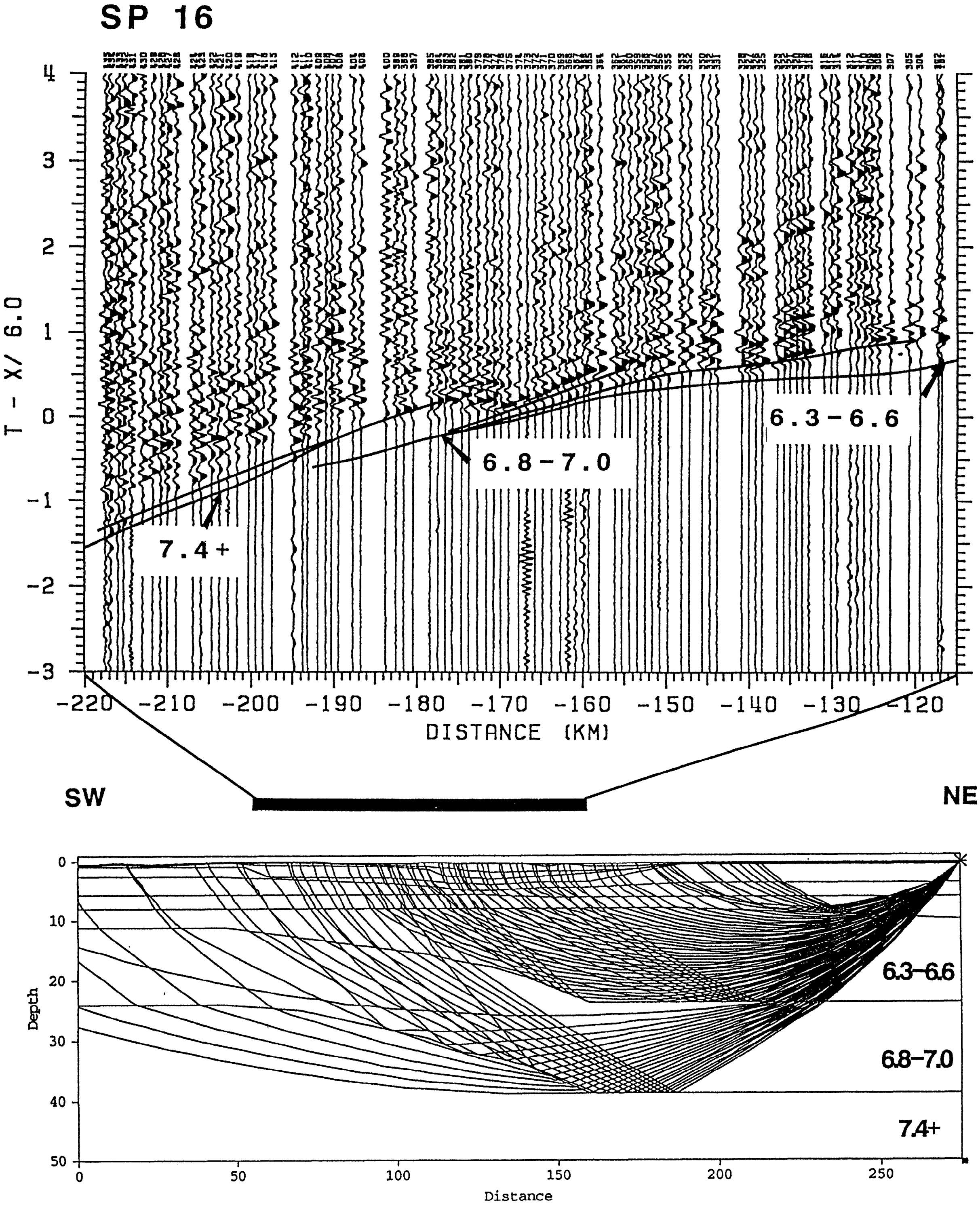

Figure 9. (top) Record section for SP 16, with travel time curves from ray trace modeling superimposed. Note that only the instrumented portion of this offset shot is shown. (bottom) The ray trace diagram for the travel time branches shown in the SP 16 record section. Note that the range of the ray trace diagram encompasses both the West Glenn and Tok Highway lines. The bar at the top of the ray trace diagram shows the spatial extent of the in-line seismic refraction data displayed above. The velocity structure northwest of SP7 is averaged from *Goodwin et al.* [1989]. The velocity structure for the Glenn Highway line at or near SP 7 cannot be projected northeastward without resulting in predicted arrival times 1-2 s earlier than those shown here. Conversely, the velocity structure developed by *Goodwin et al.* [1989] for the Tok Highway line cannot be projected southwestward without resulting in predicted arrival times 1-2 s later than those shown here.

beneath them southeast of the West Glenn line (Figure 1). Thus the greater thickness of relatively lower-velocity material observed beneath Wrangellia may postdate Peninsular-Wrangellia terrane suturing. The lower crustal structure difference may be associated with remelting and introduction of continental arc plutonic rocks.

A third explanation is that we are observing a transition within the Peninsular terrane, an intraterrane, rather than interterrane change. The 6.3+ km/s, 6.9 km/s, and deeper (?) layers may represent the Border Ranges ultramafic-mafic assemblage, at least between SPs 13 and 14. The assemblage may be closer to the surface near the southwest end of the Glenn Highway line because this section of the line is near to observed outcrops (see Figure 2). This would imply, however, that the complex is more deep-seated than previously thought from geologic mapping [*Pavlis*, 1983; *Plafker et al.*, 1989]. In addition, the Border Ranges ultramafic-mafic assemblage would appear to be thicker beneath the West Glenn line than beneath the line that crosses the Border Ranges fault to the south (see Figure 1, also *Fuis et al.* [1991]).

Comparison of Peninsular Terrane Velocity Structure to Those Determined in Other Tectonic Settings

Comparison of the velocity structure determined along the Glenn Highway line with that for "typical" continental crust of the platforms and cratons of continental interiors (Figure 10a) shows that the velocities beneath the Peninsular terrane are substantially higher at all depths greater than 8.5 km. In particular, the velocities of 6.4-6.5 km/s at 8.5-13.5 km depth and 6.9 km/s at 13.5-23 km depth are 0.3 to 0.6 km/s higher than typical continental crust at these depths. The upper crustal 6.9 km/s velocity is particularly atypical for its shallow depth, as are lower crustal velocities greater than 7.0 km/s. A crustal thickness of greater than 40 km, on the other hand, is comparable to, or slightly greater than, the average of 33-40 km found in continental interiors.

As the Peninsular terrane is thought to be a Jurassic intraoceanic island arc built on a Permian (?) basement [*Burns*, 1985; *De Bari and Coleman*, 1989], we can compare its velocity structure with that of known arc assemblages. A

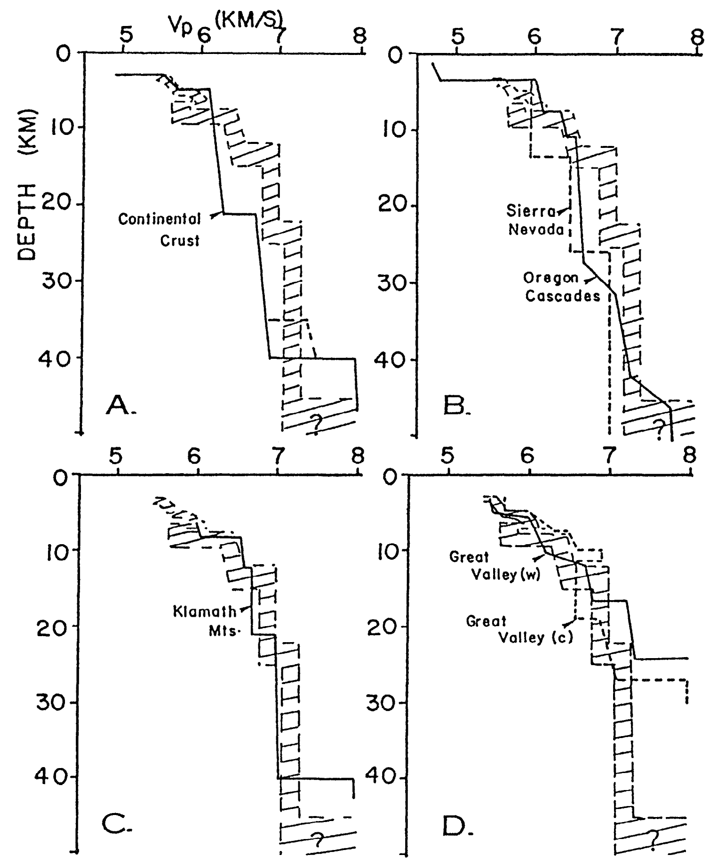

Figure 10. Comparison of the velocity-depth structure(s) derived for the in-line part of the Glenn Highway profile (hatched areas) with velocity-depth structures obtained for other representative sites. The shading of the Glenn Highway structure takes into account both the uncertainty in the interpretation at a given depth and the lateral variation in velocity at that depth. (a) Continental platform velocity structure from *Prodehl* [1984], and W. D. Mooney (personal communication, 1994). (b) Continental magmatic arc structure-Cascades volcanic arc of Oregon from *Leaver et al.* [1984] and Sierra Nevada batholith from *Eaton* [1966]. (c) Ultramafics and intraoceanic arc fragments-Klamath Mountains of northern California from *Zucca et al.* [1986] and *Fuis et al.* [1987]. (d) Forearc basin-Great Valley of California from *Colburn and Mooney* [1986] and *Holbrook and Mooney* [1987]. Solid line (western part of the Great Valley) is from *Colburn and Mooney* [1986], dashed line (central part of the Great Valley) from *Holbrook and Mooney* [1987]. Note that for all profiles, sedimentary rock thicknesses have been subtracted, so that velocity-depth profiles from other areas begin at the depth of the base of the 4.0-4.6 km/s interval.

comparison with the velocity-depth structure of the Oregon Cascades continental magmatic arc [*Leaver et al.*, 1984] (Figure 10b) shows that Peninsular terrane upper crust (3-7 km depth) appears slightly lower in velocity than the Cascades arc volcanic basement rocks at comparable depths. There is good agreement between the two curves at 7-13 km depth. From 13 to approximately 30 km, however, the Cascades model is characterized by velocities some 0.3 km/s lower than the Peninsular terrane model. Lower crustal (30-44 km) velocities appear comparable between the two locales, and maximum crustal thicknesses may also be similar (compare 44 km for the Cascades versus the greater than 40 km for the Peninsular terrane), although we do not have a well-determined Moho depth beneath the Peninsular terrane. Comparison between the Peninsular terrane model and one for the Sierra Nevada batholith in California [*Eaton*, 1966] shows a greater discrepancy in velocity structure, with velocities for the Sierra Nevada batholith lower than the Cascades model, as well as lower than the Peninsular terrane model. In summary, the Peninsular terrane model shows slightly lower to equivalent velocities in the upper crust (to 13 km depth), but higher velocities in the deeper crust than the Cascades continental magmatic arc. The Peninsular terrane exhibits higher velocities throughout the crust when compared with the Sierra Nevada batholith region.

When the Peninsular terrane model is compared to a velocity model for the Klamath Mountains (arc fragments) of California [*Fuis et al.*, 1987; *Zucca et al.*, 1986] (Figure 10c), which includes the Trinity ultramafic body of *Irwin* [1966], we observe closer agreement in velocity-depth structure than with either of the two previous comparisons. Below the 5.0-5.8 km/s upper crust, both models exhibit velocities of 6.4-6.6 km/s, the Klamath model being somewhat higher in velocity than the Peninsular terrane model. The Peninsular terrane model is some 0.2 km/s higher for most depths greater than 13 km, however. Total crustal thickness is poorly determined for both areas, but the Peninsular terrane appears thicker (40+ km) than the Klamaths (35-40 km).

The Peninsular terrane model may also be compared to those determined for the Great Valley of California [*Colburn and Mooney*, 1986; *Holbrook and Mooney*, 1987] (Figure 10d). Both regions are arc-associated and characterized by a cover of Mesozoic forearc basin sedimentary rocks and prominent aeromagnetic and gravity highs [*Grantz and Zietz*, 1960]. Above 15 km depth, velocities in the Peninsular terrane differ by no more than 0.2 km/s from the average Great Valley velocity-depth function (Figure 10d). Most significantly, both the Peninsular terrane and Great Valley models are characterized by high velocities (6.3-7.2 km/s) at relatively shallow depths (8-25 km). An important difference between the two models is that the crustal thickness beneath the Peninsular terrane is greater than that beneath the Great Valley.

Summary

This study presents some of the first information on the velocity structure beneath the Peninsular terrane in south-central Alaska and the nature of the crustal structure transition between Peninsular and Wrangellia terranes. Significant results of this study are as follows:

1. The velocity structure of the sedimentary rocks of the Copper River basin, which overlap both the Peninsular and Wrangellia terranes, is characterized by velocities ranging from 1.7 to 2.5 km/s for the Tertiary and younger strata and between 2.7 and 3.5 km/s for the Mesozoic rocks. Andesitic volcanic flows and tuffs of the Lower Jurassic Talkeetna Formation, part of the Peninsular terrane, have velocities in the 4.5 to approximately 6.0 km/s range.
2. Velocities beneath the Peninsular terrane are higher than those measured for representative continental platforms or continental magmatic arcs. Peninsular terrane velocities are similar to those determined for island arcs.
3. The mid to lower crustal structure is characterized by pronounced northeastward thickening of a 6.3-6.6 km/s layer, well to the southwest of the mapped suture between Peninsular and Wrangellia terranes. Our data from the Peninsular terrane, and the *Goodwin et al.* [1989] study for the Wrangellia terrane show that marked differences between the crustal structure beneath southern Peninsular and Wrangellia terranes persist to lower crustal (>20 km) depths.

Acknowledgments. Assistance in the seismic refraction work was provided by M. A. Daley, E. E. Criley, R. Kaderabek, P. J. Meador, W. M. Kohler, N. MacGregor-Scott, J. M. Murphy, R. H. Colburn, J. R. VanSchaack, R. A. Page, R. McClearn, D. Reneau, S. K. Gallanthine, and other U. S. Geological Survey colleagues. D. Ruggery performed some of the ray trace modeling for the 1985 SP 14 data, W. M. Kohler performed the τ-p slant stacking inversion for the 1985 SP 14 data, and B. Milkereit provided helpful suggestions regarding the implementation of the inversion procedure. J. H. Luetgert provided support of the ray trace modeling software. Song-Lin Li rechecked the matches for shot points 15 and 16. We also shared helpful discussions with D. L. Campbell on the gravity and magnetic data along the line, with E. B. Goodwin on the crustal structure of the Wrangellia terrane, and with G. Plafker, W. J. Nokleberg, A. Grantz, and R. A. Page concerning the geology and tectonics in the region. C. E. Kirschner kindly shared his knowledge of the well logging and seismic reflection data present in the Copper River basin. We are also indebted to a number of persons in public and private agencies for their generous cooperation and interest in our work. They include, for the Glenn Highway line, U.S. Bureau of Land Management (Kurt Kotter), State of Alaska (Margaret Hayes), Amoco (Robert Shaefer), and Ahtna, Inc. (Lawrence Lau). We appreciate the critical reviews by T. Brocher, R. Page, R. Clowes, K. R. Chowdhury, D. E. James, G. Wissinger, and several anonymous reviewers. The first author gratefully acknowledges the support of the NRC postdoctoral research associate program in 1984 and 1985.

References

Alaska Geological Society, Stratigraphic correlation section, Copper River basin, Alaska, 3 sheets, Alaska Geological Society, Stratigraphic Committee, Anchorage, 1969.

Andreason, E. G., A. Grantz, I. Zietz, and D. F. Barnes, Geological interpretation of magnetic and gravity data in the Copper River basin, Alaska, *U.S. Geol. Surv. Prof. Pap., 316-H*, 135-153, 1964.

Barnes, D. F., Bouguer gravity map of Alaska, scale 1:250,000, *U.S. Geol. Surv. Geophys. Invest. Map, GP-913*, 1977.

Beaudoin, B. C., G. S. Fuis, W. D. Mooney, W. J. Nokleberg, and N.I. Christensen, Thin, low-velocity crust beneath the southern Yukon-Tanana terrane, east central Alaska: results from Trans-Alaska Crustal Transect refraction/wide-angle reflection data, *J. Geophys. Res.*, *97*, 1921-1942, 1992.

Berg, E., Crustal structure in Alaska, *Tectonophysics, 20,* 165-182, 1973.

Birch, F., The velocity of compressional waves in rocks to 10 kb, 1, *J. Geophys. Res., 65,* 1083-1102, 1960.

Blank, H. R., J. H. Healy, J. Roller, R. Lamson, F. Fischer, R. McClearn, and S. Allen, Seismic refraction profile, Kingdom of Saudi Arabia: Field operations, instrumentation, and initial results, *Saudi Arabian Mission Proj. Rep. 259,* U.S. Geol. Surv., Reston, Va., 49 pp., 1979.

Blundell, D. J., The Zurich I model: How the interpretation fared, in Workshop Proceedings: *Interpretation of seismic wave propagation in laterally heterogeneous structure,* compiled by D. M. Finlayson and J. Ansorge, Bureau of Mineral Resources, Australia, pp. 177-179, 1984.

Bol, A. J., Overprint magnetization in support of northward displacement of the Chugach-Prince William terrane, Alaska, *J. Geophys. Res., 98,* 22,389-22,400, 1993.

Braile, L. W., and R. B. Smith, Guide to the interpretation of crustal refraction profiles, *Geophys. J. R. Astron. Soc., 40,* 145-176, 1975.

Burns, L. E., Gravity and aeromagnetic modelling of a large gabbroic body near the Border Ranges fault, southern Alaska, *U.S. Geol. Surv. Open File Rep., 82-460,* 1982.

Burns, L. E., The Border Ranges ultramafic and mafic complex: plutonic core of an intraoceanic island arc, 147 pp., Stanford Univ., Stanford, Ca., 1983.

Burns, L. E., The Border Ranges ultramafic and mafic complex, south-central Alaska, cumulate fractionates of island arc volcanics, *Can. J. Earth Sci., 22,* 1020-1038, 1985.

Campbell, D. L., Profiles showing models of magnetic structures in accreted terranes of south-central Alaska, scale 1:500,000, *U.S. Geol. Surv. Misc. Field Stud. Map, MF-1912,* 1987.

Campbell, D. L., and D. F. Barnes, Gravity and magnetic model of a part of the 1984 TACT line, Chugach Mountains and southern Copper River basin, in *The U. S. Geological Survey in Alaska - Accomplishments during 1984,* edited by S. Bartsch-Winkler, *U.S. Geol. Surv. Circ., 967,* 52-54, 1985.

Campbell, D. L., and W. J. Nokleberg, Magnetic profile across Denali Fault, Mount Hayes quadrangle, eastern Alaska range, in *The U.S. Geological Survey in Alaska - Accomplishments during 1983,* edited by S. Bartsch-Winkler and K. M. Reed, *U.S. Geol. Surv. Circ., 945,* 68-71, 1985.

Campbell, D. L., and W. J. Nokleberg, Magnetic model of a profile across northern Copper River basin, northeastern Gulkana quadrangle, Alaska, in *The U.S. Geological Survey in Alaska - Accomplishments during 1985,* edited by S. Bartsch-Winkler, *U.S. Geol. Circ., 978,* 35-38, 1986.

Cerveny, V., I. A. Molotkov, and I. Psencik, 214 pp., *Ray Method in Seismology,* University of Karlova, Prague, 1977.

Christensen, N. I., Seismic velocities, in *Handbook of Physical Properties of Rocks, vol. 2,* CRC Press, Boca Raton, Fla., edited by R. S. Carmichael, pp. 1-228, 1982.

Christensen, N. I., Reflectivity and seismic properties of the deep continental crust, *J. Geophys. Res., 94,* 17,793-17,804, 1989.

Christensen, N. I., M. H. Salisbury, D. M. Fountain, and R. L. Carlson, Velocities of compressional and shear waves in DSDP Leg 27 basalts, *Initial Rep. Deep Sea Drill. Proj.,* v. 27, 445-449, 1974.

Christensen, N. I., R. L. Carlson, M. H. Salisbury, and D. M. Fountain, Elastic wave velocities in volcanic and plutonic rocks recovered on DSDP Leg 31, *Initial Rep. Deep Sea Drill. Proj.,* v. 31, 607-609, 1975.

Clardy, B. I., P. T. Hanley, C. C. Hawley, and J. C. LaBelle, Guide to the bedrock and glacial geology of the Glenn Highway, Anchorage to the Matanuska Glacier and the Matanuska coal mining district, Ann. Mtg. field trip guidebook, 54 pp., *Geol. Soc. of Am., Cordilleran Sect.,* 1984.

Colburn, R. H., and W. D. Mooney, Two-dimensional velocity structure along the synclinal axis of the Great Valley, California, *Bull. Seismol. Soc. Am., 76,* 1305-1322, 1986.

Coney, P. J., D. L. Jones, and J. W. H. Monger, Cordilleran suspect terranes, *Nature, 288,* 329-333, 1980.

Csejtey, B., Jr., W. H. Nelson, D. L. Jones, N. J. Silberling, R. M. Dean, M. S. Morris, M. A. Lanphere, J. G. Smith, and M. L. Siberman, Reconnaissance geologic map and geochronology, Talkeetna Mountains quadrangle, and southwest corner of Healy quadrangle, Alaska, *U.S. Geol. Surv. Open File Rep., 78-558-A,* 60 pp., 1978.

Csejtey, B., Jr., D. P. Cox, R. C. Evarts, G. D. Stricker, and H. L. Foster, The Cenozoic Denali Fault system and the Cretaceous accretionary development of southern Alaska, *J. Geophys. Res., 87,* 3741-3754, 1982.

Daley, M. A., E. L. Ambos, and G. S. Fuis, Seismic refraction data collected in the Chugach Mountains and along the Glenn Highway in southern Alaska in 1984, *U.S. Geol. Surv. Open File Rep., 85-531,* 32 pp., 10 plates, 1985.

De Bari, S., and R. G. Coleman, The Tonsina high-pressure mafic ultramafic cumulate sequence, eastern Chugach Mountains, Alaska, *J. Geophys. Res., 94,* 4373-4391, 1989.

Eaton, J. P., Crustal structure in northern and central California from seismic evidence, in *Geology of Northern California,* edited by E. H. Bailey, *Bull. Calif. Div. Mines Geol., 190,* 419-426, 1966.

Fisher, M. A., and L. B. Magoon, Geologic framework of lower Cook inlet, Alaska, *AAPG Bull., 62,* 373-402, 1978.

Flueh, E. R., W. D. Mooney, G. S. Fuis, and E. L. Ambos, A study of peg-leg multiples from low-velocity zones in the Chugach Mountains, southern Alaska, *J. Geophys. Res., 94,* 16,023-16,036, 1989.

Fuis, G. S., and G. Plafker, Evolution of deep structure along the Trans-Alaska Crustal Transect, Chugach Mountains and Copper River Basin, southern Alaska, *J. Geophys. Res., 96,* 4229-4253, 1991.

Fuis, G. S., J. J. Zucca, W. D. Mooney, and B. Milkereit, A geologic interpretation of seismic-refraction results in northeastern California, *Geol. Soc. Am. Bull., 98,* 53-65, 1987.

Fuis, G. S., E. L. Ambos, W. D. Mooney, N. I. Christensen, and E. Geist, Crustal structure of accreted terranes in southern Alaska, Chugach Mountains, and Copper River Basin from seismic-refraction data, *J. Geophys. Res., 96,* 4187-4227, 1991.

Goodwin, E., G. S. Fuis, W. J. Nokleberg, and E. L. Ambos, The crustal structure of the Wrangellia terrane along the Tok Highway, eastern-southern Alaska, *J. Geophys. Res., 94,* 16,037-16,049, 1989.

Grantz, A., Generalized geologic map of the Nelchina area, Alaska, showing igneous rocks and large faults, scale 1:96,000, *U.S. Geol. Surv. Misc. Geol. Invest. Map I-312,* 1960.

Grantz, A., Geologic map and cross-sections of the Anchorage (D-2) quadrangle and northeasternmost part of the Anchorage (D-3) quadrangle, Alaska, *U.S. Geol. Surv. Misc. Geol. Invest. Map, I-342,* 1961.

Grantz, A., Stratigraphic reconnaissance of the Matanuska formation in the Matanuska Valley, Alaska, *U.S. Geol. Surv. Bull., 1181-I,* I1-I33, 1964.

Grantz, A., Geologic map and cross-sections of the Nelchina area, *U.S. Geol. Surv. Open File Rep. 255,* 4 sheets, 1965.

Grantz, A., and L. F. Fay, Geologic road log of the Matanuska Valley-Sutton to Caribou, in: *Guidebook, Field Trip Routes, Anchorage to Sutton, 1963, Sutton to Caribou Creek, 1964 - Oil Fields, Earthquakes, Geology,* Alaska Geological Society, Anchorage, pp. 16-22, 1964.

Grantz, A., and C. E. Kirschner, Tectonic framework of petroliferous rocks in Alaska, in: Circum-Pacific Energy and

Mineral Resources, *Mem. Am. Assoc. Pet. Geol., 25*, 291-307, 1976.

Grantz, A., and I. Zietz, Possible significance of broad magnetic highs over belts of moderately deformed sedimentary rocks in Alaska and California, *U.S. Geol. Surv. Res., 1960*, B342-B350, 1960.

Hales, A. L., and T. Asada, Crustal structure in coastal Alaska, in *The Earth Beneath the Continents, AGU Geophys. Monogr. Ser., 10*, 420-432, 1966.

Hanson, K., E. Berg, and L. Gedney, A seismic refraction profile and crustal structure in central interior Alaska, *Bull. Seismol. Soc. Am., 58*, 1657-1665, 1968.

Healy, J. H., W. D. Mooney, H. R. Blank, M. E. Gettings, W. M. Kohler, R. Lamson, and L. E. Leone, Saudi Arabian seismic deep-refraction profile: Final project report: U.S. Geol. Surv., *Saudi Arabian Mission Open File Rep. 82-37*, 429 pp. 1982.

Hillhouse, J., Paleomagnetism of the Triassic Nikolai greenstone, south-central Alaska, McCarthy quadrangle, Alaska, *Can. J. Earth Sci., 14*, 2578-2592, 1977.

Hillhouse, J., and S. Gromme, Northward displacement and accretion of Wrangellia: New paleomagnetic evidence from Alaska, *J. Geophys. Res., 89*, 4461-4467, 1984.

Holbrook, S., and W. D. Mooney, The crustal structure of the axis of the Great Valley, California, from seismic refraction measurements, *Tectonophysics, 140*, 49-63, 1987.

Hughes, D. S., and C. Maurette, Variation of elastic wave velocities in granites with pressure and temperature, *Geophysics, 21*, 277-284, 1956.

Hwang, L. J., and W. D. Mooney, Velocity and *Q* structure of the Great Valley, California, based on synthetic seismogram modelling of seismic refraction data, *Bull. Seismol. Soc. Am., 76*, 1053-1067, 1986.

Iida, K., T. Sugino, H. Furuhashi, and M. Kumazawa, Elastic dilatational wave velocity in crystalline schists from Sanbagawa metamorphic terrain, Shikoku, Japan, *J. Earth Sci. Nagoya Univ., 15*, 112, 1967.

Irwin, W. P., Geology of the Klamath Mountains province, in Geology of Northern California, edited by E. H. Bailey, *Bull. Calif. Div. Mines Geol., 190*, 19-38, 1966.

Jones, D. L., N. J. Silberling, and J. Hillhouse, Wrangellia-A displaced terrane in northwestern North America, *Can. J. Earth Sci., 14*, 2565-2577, 1977.

Jones, D. L., N. J. Silberling, H. C. Berg, and G. Plafker, Tectonostratigraphic terrane map of Alaska, *U.S. Geol. Surv. Open File Rep., 81-792*, 20 pp., 1981.

Jones, D. L., N. J. Silberling, W. Gilbert, and P. Coney, Character, distribution and tectonic significance of accretionary terranes in the central Alaska Range, *J. Geophys. Res., 87*, 3709-3717, 1982.

Jones, D. L., N. J. Silberling, P. J. Coney, and G. Plafker, Lithotectonic terrane map of Alaska, scale 1:2,500,000, in Lithotectonic Terrane Maps of the North American Cordillera, edited by N. J. Silberling and D. L. Jones, *U.S. Geol. Surv. Open File Rep. 84-523*, A1-A12, 4 sheets, scale 1:2,500,000, 1984.

Kirschner, C. E., and C. A. Lyon, Stratigraphy and tectonic development of the Cook Inlet petroleum province, in Arctic Geology, *Am. Assoc. Pet. Geol. Mem., 19*, 396-407, 1973.

Lahr, J. C., R. A. Page, C. D. Stephens, and K. A. Fogleman, Sutton, Alaska, earthquake of 1984: Evidence for activity on the Talkeetna segment of the Castle Mountain Fault system, *Bull. Seismol. Soc. Am., 76*, 967-983, 1986.

Leaver, D. L., W. D. Mooney, and W. M. Kohler, A seismic refraction study of the Oregon Cascades, *J. Geophys. Res., 89*, 3121-3134, 1984.

Liu, C., and J. M. Stock, Quantitative determination of uncertainties in seismic refraction prospecting, *Geophysics, 58*, 553-563, 1993.

Martin, G. C., The Mesozoic stratigraphy of Alaska, *U.S. Geol. Surv. Bull., 776*, 493 pp., 1926.

McClelland, W. C., G. E. Gehrels, and J. B. Saleeby, Upper Jurassic-lower Cretaceous basinal strata along the Cordilleran margin: Implications for the accretionary history of the Alexander-Wrangellia-Peninsular terrane, *Tectonics, 11*, 823-835, 1992.

McMechan, G. A., and W. D. Mooney, Asymptotic ray theory and synthetic seismograms for laterally varying structures: Theory and application to the Imperial Valley, California, *Bull. Seismol. Soc. Am., 70*, 2021-2035, 1980.

Milkereit, B., W. D. Mooney, and W. M. Kohler, Inversion of seismic refraction data in planar dipping structure, *Geophys. J. R. Astron. Soc., 82*, 81-103, 1985.

Nokleberg, W. J., W. M. Wade, I. M. Lange, G. Plafker, and D. L. Campbell, Summary of geology of northern Peninsular terrane, Gulkana River Complex, and Wrangellia terrane, north-central and northwestern Gulkana quadrangle, Alaska, in The United States Geological Survey in Alaska: Accomplishments During 1985, edited by S. Bartsch-Winkler, *U.S. Geol. Surv. Circ., 978*, 74-77, 1986.

Nokleberg, W. J., G. Plafker, J. S. Lull, W. K. Wallace, and G. R. Winkler, Structural analysis of the southern Peninsular, southern Wrangellia, and northern Chugach terranes along the Trans-Alaskan Crustal Transect, northern Chugach Mountains, Alaska, *J. Geophys. Res., 94*, 4297-4320, 1989.

Packer, D. R., and D. B. Stone, Paleomagnetism of Jurassic rocks from southern Alaska and their tectonic implications, *Can. J. Earth Sci., 11*, 976-997, 1974.

Page, R. A., G. Plafker, G. S. Fuis, W. J. Nokleberg, E. L. Ambos, W. D. Mooney, and D. L. Campbell, Accretion and subduction tectonics in the Chugach Mountains and Copper River Basin, Alaska: Initial results of the Trans-Alaska Crustal Transect, *Geology, 14*, 501-505, 1986.

Page, R. A., C. D. Stephens, and J. C. Lahr, Seismicity of the Wrangell and Aleutian Wadati-Benioff zones and the North American plate along the Trans-Alaska Crustal Transect, Chugach Mountains and Copper River basin, southern Alaska, *J. Geophys. Res., 94*, 16,059-16,082, 1989.

Panuska, B. C., D. B. Stone, and D. L. Turner, Paleomagnetism of Eocene volcanic rocks, Talkeetna Mountains, Alaska, *J. Geophys. Res., 95*, 6737-6750, 1990.

Pavlis, T. L., Pre-Cretaceous crystalline rocks of the western Chugach Mountains, Alaska: Nature of the basement of the Jurassic Peninsular terrane, *Geol. Soc. Am. Bull., 94*, 1329-1344, 1983.

Plafker, G., W. J. Nokleberg, and J. S. Lull, Bedrock geology and tectonic evolution of the Wrangellia, Peninsular, and Chugach terranes along the Trans-Alaskan Crustal Transect in the Chugach Mountains and southern Copper River basin, Alaska, *J. Geophys. Res., 94*, 4255-4295, 1989.

Plumley, P. W., R. S. Coe, T. Byrne, M. R. Reid, and J. C. Moore, Paleomagnetism of volcanic rocks of the Kodiak Islands indicates northward latitudinal displacement, *Nature, 300*, 50-52, 1982.

Plumley, P. W., R. S. Coe, and T. Byrne, Paleomagnetism of the Paleocene Ghost Rocks Formation, Prince William terrane, Alaska, *Tectonics, 2*, 295-314, 1983.

Prodehl, C., Structure in the Earth's crust and upper mantle, in *Geophysics of the Solid Earth, the Moon and the Planets*, vol. V-IIA, Springer-Verlag, New York, pp. 97-206, edited by K. Fuchs and H. Soffel, 1984.

Saleeby, J. B., Accretionary tectonics of the North American Cordillera, *Annu. Rev. Earth Planet. Sci., 15*, 45-73, 1983.

Shaw, P. R., Quantitative comparison of seismic data sets with waveform inversion: Testing the age-dependent evolution of crustal structure, *J. Geophys. Res., 97*, 19,981-19,991, 1992.

Stephens, C. D., K. A. Fogleman, J. C. Lahr, and R. A. Page, The Wrangell Benioff zone, southern Alaska, *Geology, 12*, 373-376, 1984.

Stone, D. B., and D. R. Packer, Tectonic implications of Alaska Peninsular paleomagnetic data, *Tectonophysics, 37*, 183-201, 1977.

Walder, J. and A. Nur, Porosity reduction and crustal pore pressure development, *J. Geophys. Res., 89*, 11,539-11,548, 1984.

Walter, A. W., and W. D. Mooney, Crustal structure of the Diablo and Gabilan ranges, central California: A reinterpretation of existing data, *Bull. Seismol. Soc. Am., 72*, 1567-1590, 1982.

Wilson, J. M., Supplementary data report (magnetic tape) for Open-File 85-531: 1984 TACT seismic refraction survey, south-central Alaska, *U.S. Geol. Surv. Open File Rep., 87-482*, 3 pp., 1 mag. tape, 1987.

Wilson, J. M., P. Meador, and G. S. Fuis, Data Report for the 1985 TACT seismic refraction survey, south-central Alaska, *U.S. Geol. Surv. Open File Rep. 87-440*, 78 pp., 1 mag. tape, 1987.

Winkler, G. R., M. L. Silberman, A. Grantz, R. J. Miller, and E. M. MacKevett, Jr., Geologic map and summary geochronology of the Valdez quadrangle, southern Alaska, *U.S. Geol. Surv. Open File Rep., 80-892-A*, 1981.

Wolf, L. W., D. B. Stone, and J. N. Davies, Crustal structure of the active margin, south central Alaska: an interpretation of seismic refraction data from the Trans-Alaska Crustal Transect, *J. Geophys. Res., 96*, 16,455-16,469, 1991.

Woollard, G. P., N. A. Ostenso, E. Thiel, and W. E. Bonini, Gravity anomalies, crustal structure, and geology in Alaska, *J. Geophys. Res., 65*, 1021-1037, 1960.

Zelt, C. A., and R. B. Smith, Seismic traveltime inversion for 2-D crustal velocity structure, *Geophys. J. Int., 108*, 16-34, 1992.

Zucca, J. J., G. S. Fuis, B. Milkereit, W. D. Mooney, and R. D. Catchings, Crustal structure of northeastern California, *J. Geophys. Res., 91*, 7359-7382, 1986.

E. L. Ambos, Department of Geological Sciences, California State University at Long Beach, 1250 Bellflower Boulevard, Long Beach, CA 90840. (e-mail: bambos@beach.csulb.edu)

G. S. Fuis and W. D. Mooney, U.S. Geological Survey, MS 977, 345 Middlefield Road, Menlo Park, CA 94025.

(Received March 4, 1994; revised August 19, 1994; accepted September 30, 1994.)